Development of electrical on-mask CD test structures based on optical metrology features

Development of Electrical On-Mask CD Test Structures Based on Optical Metrology Features

A. Tsiamis*, S. Smith*, M. McCallum†, A.C. Hourd‡, O. Toublan§, J.T.M. Stevenson* and A.J. Walton*
*Institute of Integrated Micro and Nano Systems, School of Engineering and Electronics,
Scottish Microelectronics Centre, The University of Edinburgh, Kings Buildings, Edinburgh, EH9 3JF, U.K.
Email: A.Tsiamis@ed.ac.uk
†Nikon Precision Europe GmbH, Appleton Place, Appleton Parkway, Livingston, West Lothian, EH54 7EZ, U.K.
‡Compugraphics International Ltd., Eastfield Industrial Estate, Glenrothes, Fife, KY7 4NT, U.K.
§Mentor Graphics (Ireland) Ltd., French Branch, 180 Av de l'Europe,
ZIRST de Montbonnot, 38334 ST ISMIER CEDEX, France

***Abstract*— The standard approach to generate the data required for automated proximity correction is to measure a set of patterned features using an optical tool or a critical dimension scanning electron microscope (CD-SEM). This paper describes the design of a set of on-mask electrical test structures to perform the same task which has a number of attractions. The electrical test structures are based on the Kelvin bridge resistor to measure the widths of isolated and densely packed lines and spaces. The results from these measurements can be used to extract information about proximity effects in the mask making process and to generate rules or models for the correction of mask designs. Electrical results from a test mask, fabricated without any correction for e-beam proximity effects, are presented and compared with optical measurements of the same structures made with an industry standard mask metrology tool.**

I. Introduction and Background

Previous publications have demonstrated the usability of on-mask electrical test structures for sheet resistance and critical dimension (CD) characterisation. Electrical CD results obtained from alternating aperture phase shifting masks (Alt-PSMs) have been presented and compared favourably with measurements made on the same test structures using a CD-SEM [1], [2], AFM [3]–[6] and more recently optical tools [7]. The present work attempts to extend this by adapting industry standard optical test sites into electrically measured, on-mask test structures. A number of structures have been designed and fabricated on a mask plate and results from electrical and optical measurements made on these are presented.

II. Test Structures

A. Optical Test Structures

The starting point for this work is a set of industry standard on-wafer metrology test patterns provided by Mentor Graphics (MG), which can be measured optically or by CD-SEM. Figure 1 illustrates part of the MG test set. Isolated and densely packed line arrangements are used for improving tool calibrations in linewidth and line-spacing metrology and for investigating proximity distortion effects. This in turn helps to determine the rules and calculate the parameters required for proximity correction schemes. In addition experimental data taken from measurements on such patterns, are used to optimise optical lithography process simulation models. By adapting the test set for photomask metrology similar information can extracted for the mask making process. Furthermore real reference data can be used at the mask step of the lithographic models, which typically do not take in to account mask effects but assume perfect dimensions and conditions for the mask as defined in the CAD data.

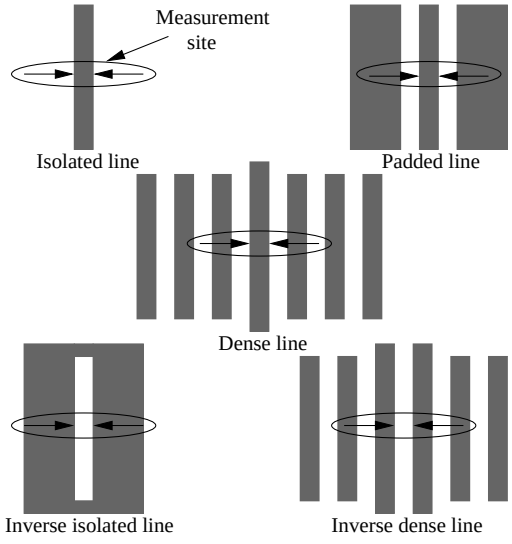

Fig. 1. Examples of optical metrology features.

B. Electrical Test Structures

A prototype binary mask (MSN5757) was fabricated to investigate the proposed measurement test sites. It includes on-mask, electrical test structures based on the well understood cross-bridge resistor [8] and an extension of it, termed the split-cross bridge resistor [9]. The test structures are patterned into the conductive chrome layer of the photomask and their layout is illustrated in figure 2. To provide clear and unambiguous information about the capability of the fundamental mask making process, this mask has been written without any of the correction strategies usually applied for manufacture.

The mask layout (see figure 3(a)) contains 9 blocks of identical test structures (A1-C3) and two blocks of large pad printable test structures designed to be measurable when reduced by a 4X photolithography system. Each block (see figure 3(b)) consists of 108 structures which are split into 9 sets of 12 structures and are capable of characterising the feature arrangements presented in figure 1. Seven sets consist of

isolated and dense cross-bridge resistors with nominal widths (W_B) ranging from 480 to 4800nm. The two remaining sets consist of isolated and dense split-cross-bridge structures with nominal line-spacings (S) ranging from 480 to 4800nm. The dimensions of the on-mask features are four times larger than those in the MG test set, which are defined for on-wafer metrology.

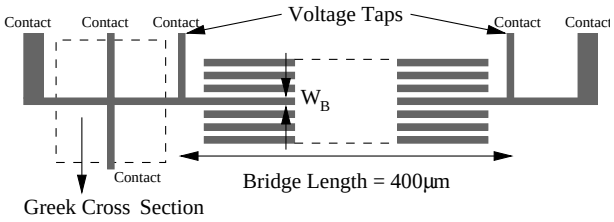

(a) Cross-bridge test structure for dense features

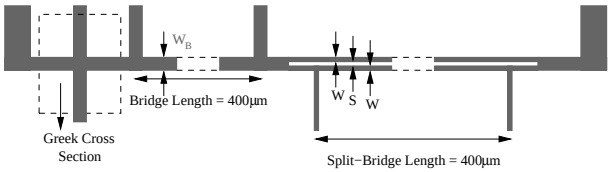

(b) Split-cross-bridge test structure for inverse isolated lines

Fig. 2. Partial schematic layouts of test structures.

III. Electrical and Optical CD Measurement Techniques

The optical and electrical measurement techniques used to extract the CDs of the structures on mask MSN5757 are presented in detail below.

A. ECD Measurement

To extract the electrical linewidth from an on-mask chrome cross-bridge test structure, firstly the sheet resistance (R_S) is measured at the heart of the Greek cross section. This is done by forcing a current between two adjacent arms of the cross (A and B in figure 4) and measuring the voltage between the other two (C and D). The procedure is repeated with the current flow reversed, to highlight any instrumentation offsets introduced by the measurement equipment. In addition the two measurements are repeated in a 90° orientation (i.e. the current forcing terminals are rotated by 90° and current is forced between B and C) to highlight any asymmetries in the geometry of the Greek cross. Finally the results of the four Kelvin resistance measurements are averaged (R_{avg}) and the sheet resistance is calculated using [10]

$$R_S = \frac{\pi R_{avg}}{\ln 2} \tag{1}$$

This equation is used if the structure displays 90° rotational symmetry [11]. Otherwise a correction factor (f) is calculated and applied to reduce any error introduced by the asymmetries in the Greek cross [10].

Next the resistance (R_B) of the four terminal bridge section is measured. A current is forced from one end of the structure to the other and the resistance of the bridge is calculated from the voltage measured at the voltage taps (see figure 4). The ECD of the line can then be extracted by using [8]

$$W_B = \frac{R_S L_B}{R_B} \tag{2}$$

where L_B is the length of the bridge section between the centers of the voltage taps.

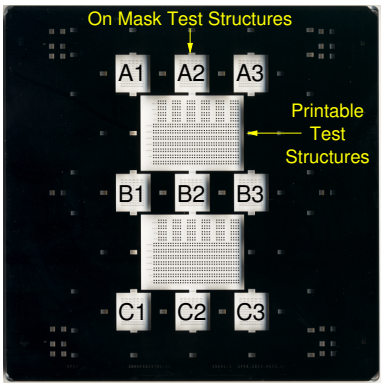

(a) Layout of binary mask (MSN5757).

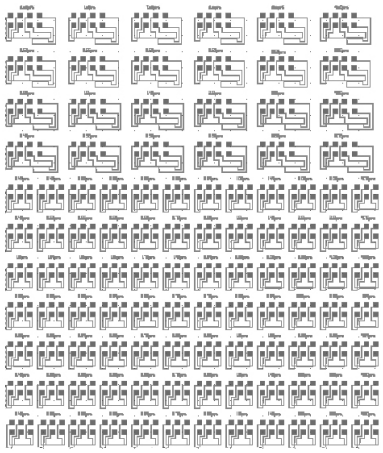

(b) Expanded view of a block of on-mask test structures.

Fig. 3. Layout of binary mask (MSN5757) with a close up view of one block of on-mask test structures.

B. OCD Measurement

To optically measure an on-mask feature, an image of the feature is captured by the transmission of light through the photomask. The image data are then processed to generate an intensity profile for the area where the measurement is to be made. The linewidth is measured by applying a set threshold that determines the edges of the feature from the points at which the intensity crosses the threshold. Finally the feature width is calculated as the difference between the edge positions.

Although CD metrology using optical microscopy has traditionally used threshold algorithms for calculating the edge position, they are usually non-linear in linewidth (in particular for small features) and suffer from optical proximity effects

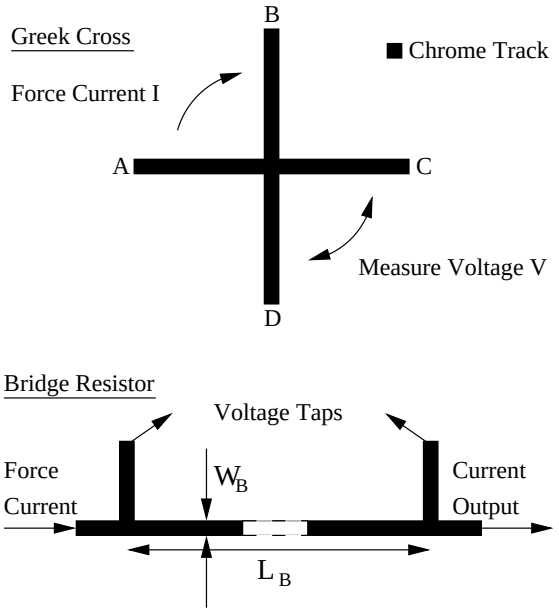

Fig. 4. Schematic layouts of binary Greek cross sheet resistance and Kelvin bridge resistor structures.

(OPE). For this reason correction offsets have to be applied to compensate for the errors introduced with the optical measurement. These errors are corrected with the use of multi-point calibration techniques, each appropriate to the type, density and dimension of the feature being measured. These corrections are usually determined from measurements made on reference test sites, which unfortunately can become complicated and impractical.

IV. Measurements and Results

Electrical measurements on mask MSN5757 were made using an HP4062B Semiconductor Parametric Test System and a high resolution Solartron 7065 voltmeter. The Solartron has a 1μV sensitivity on a range of $\pm$10mV, which is within the voltage sensing resolution requirements of this work. In addition the accuracy of the tool is within $\pm 0.001\%$ of the measured voltage. Optical measurements were made with a 248nm DUV (MueTec <M5k>) dedicated photomask CD metrology system [12]. This tool has been extensively characterised in a reticle production environment and demonstrated the ability to resolve sub-100nm chrome lines, with a usable measurable line and space resolution down to 200nm [12]. Electrical and optical results from mask MSN5757 are presented below.

A. Short and Long-Term Measurement Repeatability

To test the repeatability of the electrical measurement technique the ECDs of isolated lines were measured ten times, with the test structures being reprobed for each measurement. A current of 500μA was chosen as this gave the lowest short term standard deviation (σ), for currents between 10μA and 1mA. This is less than 0.4nm or a 0.05% variation, for structures with nominal CD values between 480nm and 4800nm. For long-term stability testing the electrical CDs were sequentially measured ten times each day for five consecutive days, with the structures being reprobed each day. This gave a σ_{ECD}<0.8nm, i.e. less than 0.08% variation. Whilst five days have been deemed a long-term period for the purposes of this work, repeatability verification in an industrial production environment would normally require many weeks of testing, with many measurement cycles performed each day.

Optical CD measurements were repeated three times on the same structures and gave a short-term σ_{OCD}<0.5nm for all dimensions, i.e. a variation below 0.1% for all measured linewidths. Although optical long-term repeatability testing was not performed using mask MSN5757, reference [12] reports a $3\sigma_{OCD}$<0.5nm for submicron isolated lines on a binary chrome-on-glass mask measured with the same <M5k> tool.

B. Isolated Lines

Electrical and optical CDs have been measured from one set (part of block B2) of isolated structures. The measured linewidths have been subtracted from the designed dimensions and the results are presented in figure 5. All of the isolated lines appear narrower than the designed CDs but the optical and electrical results do not show the same trends. ECD results suggest that there is a non-linear transfer in linewidth for sub-micron designed widths, which could be attributed to the exposure of the resist or the etching of the chrome being non-linear in linewidth. On the other hand for nominal widths <720nm the optical results indicate an increase in feature size as the design width decreases.

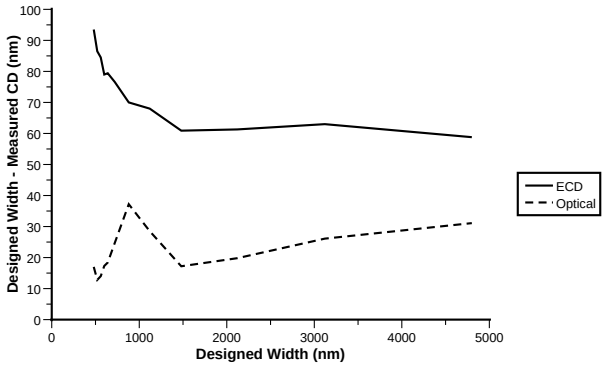

Fig. 5. Comparison of ECD and optical results from isolated structures for a range of dimensions.

The optical measurements depend on the ability to obtain accurate images from which to extract the width of the features. The results suggest that this is not the case for the narrowest features, although they can be clearly resolved. One possible reason for this is that for narrow isolated features the light intensity range is reduced, however the percentage threshold is still applied. This shifts the threshold upwards in the intensity curve to a level that positions the edges of the feature at a greater distance between them making the line appear wider.

Although a multi-point calibration for isolated features has been applied to the optical tool used for these measurements, the reference mask used only allows the calibration of linewidths $\geq$700nm and this is directly reflected in the results. The electrical CD offset is almost constant for dimensions wider than 1.5μm, while the optical offset increases with the designed width. This again suggests that the optical tool requires better calibration.

C. Dense Lines

The electrical and optical linewidths for one set of dense structures were extracted and the results for 600nm wide lines are shown in figure 6. For line-spacings $>$1.5μm, the ECD and optical results track each other well with a nearly constant offset ($<$2nm variation for both types of measurements). The proximity of neighbouring features which are separated by over 1.5μm does not appear to affect the CD and so dense line formations at such distances can be considered isolated.

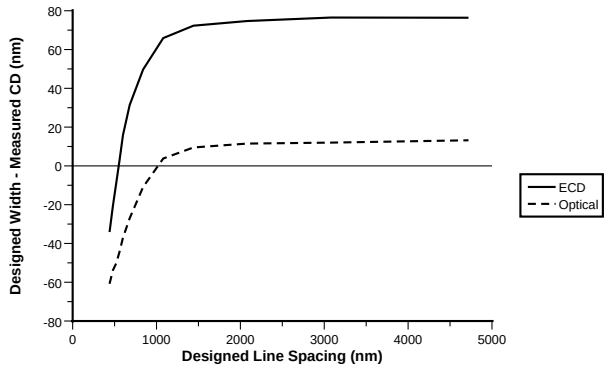

Fig. 6. Comparison of ECD and optical results from 600nm wide dense structures for a range of line to space ratios.

For structures with line-spacings $<$1.5μm the CD offset decreases as the line-spacing decreases up to the point where lines appear wider than the nominal width. This is an indication that the proximity of the neighboring features is having an effect on the CD. In addition, it can be observed that the offset between the optical and electrical measurements does not remain constant when the spacing is below 800nm. The electrical measurements indicate how proximity effects alter the dimensions of the features during the mask fabrication process, while for the optical technique this effect is also confounded with the optical measurement itself. In particular proximity effects caused by the convolution of the intensity profiles of adjacent lines introduce errors in the determination of the line edge location and thus the measured OCD [13].

Calibration offsets have to be applied to the optical tool to correct for these effects. It should be noted that in this case the calibration reference plate used does not contain any dense features and so should be considered raw data. The ECD results show that the measured lines are wider than their design width when the line-spacing is less than the nominal width of the lines. In other words when the line to space ratio of the dense pattern is greater than unity, the measured lines are electrically wider than designed. It can also be observed that with optical measurements dense lines with spacings below $\sim$1μm appear to be wider than the nominal CD.

D. Inverse Isolated Lines - Split Bridge Structures

The line-spacing in the split bridge structures can be measured directly with the optical tool. The electrical measurement is more complicated and both the solid bridge width (W_b) and the widths of the two half lines (W) are required (the method presented in section III-A is also used for the measurement of the split-lines). The line-spacing S is then $W_b - 2W$. Optical and electrical line-spacing results from one set of inverse isolated structures are presented in figure 7.

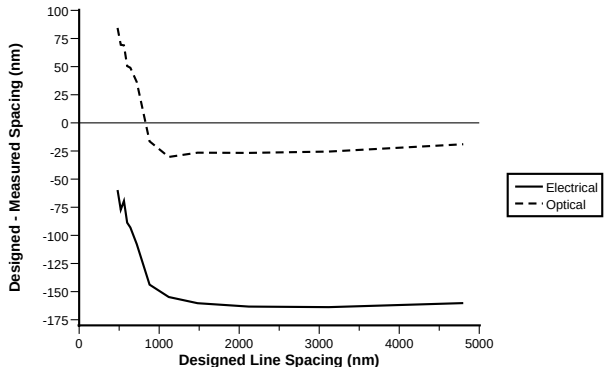

Fig. 7. Comparison of electrical and optical line-spacing results.

For nominal line-spacing larger than 880nm the measured values appear wider than designed for both measurement methods. Furthermore, for spacing dimensions $>$1.5μm the offset is almost constant. For nominal spacing values $<$880nm there is a rapid change in the offset as dimensions reduce, but the difference between the optical and electrical measurements remains constant. For both results the extracted spacings get narrower as dimensions reduce. This is due to proximity effects between the internal sides of the abutting tracks forming the spacing. This effectively increases the fabricated width of the lines but decreases their line-spacing. One interesting thing to note is that both techniques detect a change in the trends of the curves between 520nm and 560nm spacings. This is most clear in the electrical results and most likely represents a real effect on the mask.

E. Inverse Dense Lines - Split Bridge Structures

The inverse dense set consists of dense line features with varying linewidths. The nominal line-spacing between the split-lines (and between the surrounding dummy lines) is 520nm for all structures. The split-lines are the two abutting half-lines of each structure defining the line-spacing under investigation. Optical and electrical line-spacing results from one set of inverse dense structures (that of block B2) are presented in figure 8.

Both measurement techniques show the measured line-spacing to be narrower than the nominal value; however, the offset between the two methods is not constant except for

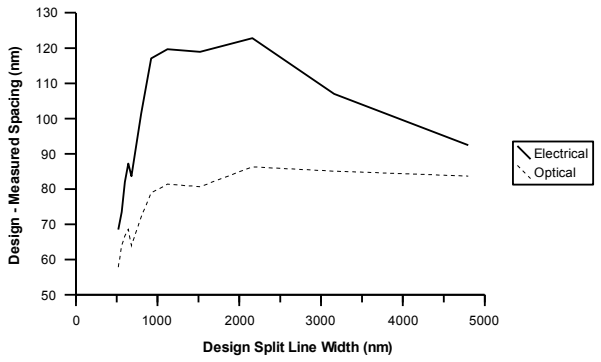

Fig. 8. Comparison of electrical and optical line-spacing results from dense structures.

a small range of split-linewidths. It can be seen that for sub-micron split-lines the offset between the measured line-spacing and the design target decreases as the width of the split-lines decreases. Since the nominal line-spacing remains constant for all structures, the split-line to space ratio decreases as the width of the split-line decreases. Split-lines with smaller split-line to space ratio appear more narrow (from the nominal) than the lines with a higher ratio. This in turn makes the measured line-spacing appear wider, causing the decrease in the offset observed in figure 8. The unexpected change in the trend between 680nm and 640nm tracks is most likely caused by a local effect on the mask and not a measurement error, as it has been detected by both measurement techniques.

In addition, for sub-micron split-lines the line-spacing offset between the two measurement techniques is not constant, but increases as the split-lines get wider. This effect is similar to the CD offset variations observed with the dense lines of section IV-C. For the optical measurement the determination of the location of the edges of a line or space feature and consequently the measured OCD, is affected by the proximity of adjacent feature edges.

It is only for linewidths between 920nm and 2160nm that the curves of figure 8 track each other reasonably well and with a nearly constant offset. For split-lines wider than 2160nm the optical line-spacing offset seems to level to a nearly constant value ($<$2nm variation). This is expected since the split-lines have become wide enough that further increases in their linewidth does not alter the effect they have on the dimensions of the spacing between them.

This is not the case for the electrical results, where the offset reduces significantly. This effect is almost certainly caused by the isolated bridge which has been used as a reference for the electrical calculation of the line-spacing. The calculation assumes that the outer width of the split-lines is the same as that of the solid bridge line. This is not the case here as the split-lines are surrounded by dummy features. There are proximity effects on the inner and outer edges of the split-lines although the line-spacing calculation should only depend on the inner sides of the split-lines which become wider. The proximity of the outer edges of the split-lines with the dummy features alters the outer width of the fabricated split-lines in a different manner to that of the reference bridge line. Therefore, the trend of the electrical line-spacing is masked by the above effect for these dimensions and the optical results can be trusted more confidently. This design error has been modified for the next mask, which includes proximity corrections and initial results suggest that the two techniques track each other.

V. Conclusions and Further Work

A set of optical measurement reference test sites formed the basis for the design and fabrication of on-mask electrical test structures used for CD and line-spacing metrology. Electrical and optical measurements were made and the results suggest that the electrical technique is not affected by the dimensions or the proximity of the features, unlike the optical method. This is very important as effects seen when electrically characterising a feature can more confidently be attributed to the mask fabrication process and not to the measurement technique. A second mask with proximity correction for e-beam lithography by equalisation of background dose (GHOST) [14] has been fabricated. The structures of the two masks will be compared electrically and optically to investigate the effectiveness of compensating for proximity effects. This will prove a valuable tool for optimising the correction rules and models applied when manufacturing masks. Furthermore, it will provide additional information on the effectiveness of the electrical and optical measurement techniques.

Acknowledgements

The authors would like to acknowledge the support of the Edinburgh Research Partnership, EPSRC (GR/S12838/01), Nikon, Compugraphics and Mentor Graphics.

References

[1] S. Smith, M. McCallum, A. Walton, and J. Stevenson, "Electrical CD Characterisation of Binary and Alternating Aperture Phase Shifting Masks," in *Proceedings of IEEE International Conference on Microelectronic Test Structures*, Cork, Ireland, April 2002, pp. 7–12.

[2] S. Smith, M. McCallum, A. Walton, J. Stevenson, and A. Lissimore, "Comparison of Electrical and SEM CD Measurements on Binary and Alternating Aperture Phase-Shifting Masks," *IEEE Transactions on Semiconductor Manufacturing*, vol. 16, no. 2, pp. 266–272, May 2003.

[3] S. Smith, M. McCallum, A. Walton, J. Stevenson, P. Harris, A. Ross, A. Hourd, and L. Jiang, "Test Structures for CD and Overlay Metrology on Alternating Aperture Phase-Shifting Masks," in *Proceedings of IEEE International Conference on Microelectronic Test Structures*, Awaji Yumebutai International Conf. Center, Japan, March 2004, pp. 22–25.

[4] M. McCallum, S. Smith, A. Hourd, A. Walton, and J. Stevenson, "Cost Effective Overlay and CD Metrology of Phase-Shifting Masks," in *Proceedings of the SPIE, Vol. 5567: 24th Annual BACUS Symposium on Photomask Technology*, 2004, pp. 22–25.

[5] S. Smith, M. McCallum, A. Walton, J. Stevenson, P. Harris, A. Ross, and L. Jiang, "On-Mask CD and Overlay Test Structures for Alternating

Aperture Phase Shift Lithography," *IEEE Transactions on Semiconductor Manufacturing*, vol. 18, no. 2, pp. 238–245, May 2005.

[6] S. Smith, A. Walton, M. McCallum, A. Hourd, J. Stevenson, A. Ross, and L.Jiang, "Improved Test Structures for the Electrical Measurement of Feature Size on an Alternating Aperture Phase-Shifting Mask," in *Proceedings of IEEE International Conference on Microelectronic Test Structures*, K.U. Leuven, Leuven, Belgium, April 2005, pp. 17–22.

[7] S. Smith, A. Tsiamis, M. McCallum, A. Hourd, J. Stevenson, and A. Walton, "Comparison of Optical and Electrical Measurement Techniques for CD Metrology on Alternating Aperture Phase-Shifting Masks," in *Proceedings of IEEE International Conference on Microelectronic Test Structures*, Austin, Texas, USA, March 2006, pp. 119–123.

[8] M. Buehler, S. Grant, and W. Thurber, "Bridge and van der Pauw Sheet Resistors For Characterizing the Line Width of Conducting Layers," *J. Electrochemical Soc - Solid State Technology*, vol. 125, no. 4, pp. 650–654, April 1978.

[9] M. Buehler and C. Hershey, "The Split-Cross-Bridge Resistor for Measuring the Sheet Resistance, Linewidth, and Line Spacing of Conducting Layers," *IEEE Transactions on Electron Devices*, vol. ED-33, no. 10, pp. 1572–9, Oct 1986.

[10] M. Buehler and W. Thurber, "An Experimental Study of Various Cross Sheet Resistor Test Structures," *J. Electrochemical Soc - Solid State Technology*, vol. 125, no. 4, pp. 645–650, April 1978.

[11] S. Smith, A. Walton, and M. Fallon, "Investigation of Optical Proximity Correction (OPC) and Non-Uniformities on the Performance of Resistivity and Linewidth Measurements," in *Proceedings of IEEE International Conference on Microelectronic Test Structures*, Göteborg, Sweden, March 1999, pp. 161–166.

[12] A. Hourd, A. Grimshaw, G. Scheuring, C. Gittinger, S. Döbereiner, F. Hillman, H.-J. Brück, S.-B. Chen, P. Chen, R. Jonckheere, V. Philipsen, H. Hartmann, V. Ordynskyy, K. Peter, T. Schätz, and K. Sommer, "Reliable sub-nanometer repeatability for CD metrology in a reticle production environment," in *Proceedings of the SPIE, Vol. 4889: 22nd Annual BACUS Symposium on Photomask Technology*, 2002, pp. 319–327.

[13] N. Doe and R.Eandi, "Optical proximity effects in submicron photomask CD metrology," in *Proceedings of the SPIE, Vol. 3996: 16th European Conference on Mask Technology for Integrated Circuits and Microcomponents*, February 2000, pp. 139–154.

[14] G. Owen and P. Rissman, "Proximity effect correction for electron beam lithography by equalization of background dose," *Journal of Applied Physics*, vol. 54, no. 6, pp. 3573–3581, June 1983.